Journal of Earthquake and Tsunami
(2020)

DOI: 10.1142/S1793431120500086

The Effect of the Mainshock–Aftershock on the Estimation of the Separation Gap of Regular and Irregular Adjacent Structures with the Soft Story

Mostafa Khatami*, Mohsen Gerami† and Ali Kheyroddin‡
Faculty of Civil Engineering, Semnan University, Semnan, Iran
*m_khatami@semnan.ac.ir
†mgerami@semnan.ac.ir
‡kheyroddin@semnan.ac.ir

Navid Siahpolo
Department of Civil Engineering
Academic Center for Education, Culture, and
Research, Khouzestan, Iran
n.siahpolo@gmail.com

Received 10 August 2019
Accepted 3 October 2019
Published 6 December 2019

One way for decreasing the effect of pounding is to set the separation gap between two adjacent buildings. On the one hand, earthquakes in earthquake-prone zones often occur as a chain of successive earth movements in the form of foreshock, mainshock and aftershock. On the other hand, the existence of soft story in the lowest story of the structure is the most common type of irregularity in lateral stiffness. This paper investigates the effect of seismic sequences to estimate the separation gap at the highest collision level of two adjacent structures. For this purpose, 335 adjacent combinations of regular and irregular steel moment-resisting frames are evaluated which have a soft story on the first story. Separation gap demand is calculated using dynamic analysis of nonlinear time history under a set of seismic sequences which are a combination of the mainshock and aftershock. Results of the total of analysis done show the seismic sequence effects are significant and should be considered in the process of determining the normal separation gap (here after, NSG). Finally, based on the done studies, an empirical relationship is presented to estimate the seismic sequence effects on separation gap of two regular and irregular adjacent structures.

Keywords: Seismic sequence; mainshock–aftershock; soft story; adjacent combination; normal separation gap.

1. Introduction

The impact was a dynamic phenomenon with severe nonlinear behavior which was caused by the pounding of two structures with each other when lateral forces were

† Corresponding author.

applied. Created forces during the pounding occurred in a short time and led to the total destruction of the structure or partial destruction of the structure. This phenomenon was not considered in the current design, and design codes usually proposed a suitable separation gap between two structures to prevent its effects on adjacent structures [Shehata and Raheem, 2014; Hatzigeorgiou and Pnevmatikos, 2014].

Several research works have been carried out to calculate the necessary separation gap to prevent the pounding of the adjacent frames. Shrestha's [2013] research showed that the spectral difference method estimated the amount of the necessary separation gap for adjacent structures in comparison with the method of sum of absolute displacements and Square-Root-of-Sum-of-Squares (SRSS) of lateral displacement with high precision. Efraimiadou *et al.* [2013a] examined the impact of irregular adjacent buildings which had a setback. The results showed that the time history of lateral displacement and the separation gap had the dependency on the way of arrangement of the frames adjacent to each other and the irregularity amount. Hao [2015] examined the effects of applied non-uniform earthquakes on supports due to the wave propagation from inside the soil and its dependency on the soil type. The results showed that ignoring the effects of non-uniform earthquakes led to an underestimation of the separation gap demand of the two structures in the range of equal vibration frequencies. Naderpour *et al.* [2017] with the help of the artificial neural network proposed a new relationship to the separation gap. This relationship, which was based on the maximum lateral displacement and the period time of two structures, could be used to estimate the separation gap with high precision between structures with different period times. Favvata [2017] investigated the minimum gap required for the pounding of adjacent reinforced concrete frames with different heights of the first story under three seismic hazard levels. The results showed that this minimum gap depended on the limit state and the seismic hazard level that was considered for evaluation.

On the one hand, seismic design code of structures, such as ASCE/SEI 7-16 [2016], only considered a specific earthquake, which is called design earthquake, to analyze and design structures against earthquakes. On the other hand, according to past experiences in the seismic area, after the main earthquake, a series of aftershocks with different magnitudes and a different time interval occurred due to static and dynamic stresses during the earthquake process. Aftershocks had the potential of high damage in the structure because, firstly, the situation of their occurrence (the distance from the center to the situation of the affected structures) and the released energy content were not predictable. Secondly, the damaged structures of the main earthquake had less stiffness capacity and less resistance capacity under the influence of aftershocks. The effect of these aftershocks on the structure, especially in the case of the pounding of adjacent structures, was ignored in the seismic design codes, and the seismic sequence effects were not included in the proposed separation gap warrants of the codes [Abdelnaby, 2012; Mantawy, 2014].

Among the research works carried out so far on the effects of seismic sequences, the research of Garcia [2012] can be mentioned. The results showed that the effect of seismic sequences on the seismic demands of the structure (lateral displacement, drift, and residual drifts) was significant in the case where the period time of the aftershock and the period time of the first mode of the studied structure were close to each other. Zhai *et al.* [2012] studied the time history of the inelastic response of a system with a single degree of freedom under sequential earthquakes. The results showed that aftershocks might increase the lateral displacement of the structure or change the residual displacement. The ratio of maximum displacement of the structure under aftershocks to maximum displacement under the main earthquake was more than 60% in most investigated cases. Faisal *et al.* [2013] examined demands of the story ductility (the resulted maximum drift of nonlinear analysis of time history to the drift of yield point of nonlinear static analysis) in inelastic concrete frames subjected to sequential earthquakes. The results showed that with increasing the period time of structures and increasing their behavior factor, the maximum demand of the story ductility under the seismic sequence was greater than that of under single earthquake. Hatzivassiliou and Hatzigeorgiou [2015] evaluated the effects of actual seismic sequence with a vertical component of the earthquake on 3D regular and irregular structures. The displacement of the highest story, the residual displacement and the ductility demand in the seismic sequence increased compared to the single earthquake. The structural demand increase was highly dependent on the irregularity of the structure in height, the specification of the 3D structural model and the method of applying seismic loading. Hosseinpour and Abdelnaby [2017] showed that earthquake direction in irregular buildings, structural irregularities, and earthquake vertical component had a significant effect on the response of the structure under seismic sequence.

Limited studies were done on the effects of impact on irregular adjacent buildings under the influence of consecutive earthquakes. Efraimiadou *et al.* [2013b] showed that earthquake records' sequences led to an increase in the lateral displacement of stories relative to the state of the single earthquakes, which would result in increasing the separation gap amount. So, lateral displacement in 67.4% of studied adjacent combinations was more than 20% higher than that obtained from singular earthquakes. The probabilistic evaluation was done by Nazri *et al.* [2018] on irregular adjacent structures in height (which had setback) under successive seismic stimulation. Results showed that in order to avoid a soft-story failure, the column stiffness had to be increased, especially in the first story.

According to the occurrence of seismic sequence in different parts of the world and few studies regarding its effect on the impact of adjacent structures and the separation gap demand, especially in irregular structures in height, this paper, tryies to provide an empirical relationship regarding seismic sequence effects on the estimated separation gap of regular and irregular adjacent structures with soft stories at the first story based on accurate and sufficient analyzes.

2. The Studied Frames

The modeled frames were two-dimensional steel moment frames with high ductility (special). The number of their stories was considered 2, 4, 6, 8, 10, 12, 14, 16, 18 and 20 stories. The frames had three spans. The lengths of the spans were fixed and equal to 5.5 m. In regular frames, the height of all stories was equal to 3.5 m. To create the irregularity in lateral stiffness on the first story, the height of the stories was considered to be 4.5 m and 5.5 m (in irregular models). These models were classified as a building with a very soft story (extreme soft story irregularity), according to Table 12.3–2 of section 12.3 of ASCE/SEI 7-16 and Iranian Standard No. 2800 (4th edition) [2014]. Thirty regular and irregular frames had been loaded with gravity load in accordance with Iranian National Building Code: Design Loads for Buildings-Division 6 [2014]. In gravity loading, the dead and live loads of the stories were 650 kgf/m^2 and 250 kgf/m^2, respectively, with a loading width of 5 m. The mass of all stories was assumed the same. The seismic loading of frames was based on Iranian Standard No. 2800. In seismic loading, the mass of stories was calculated from the dead loads plus 20% of the live loads (DL + 20% LL). The soil of the construction site was considered type III. The relative risk of the earthquake of the construction site was very high. Usage type was residential with a degree of medium importance.

All the frames were analyzed based on the equivalent-static analysis using the ETABS software [2015]. Then, they were designed in accordance with the load and resistance factor method [Iranian National Building Code: Design and Construction of Steel Structures-Division 10, 2014]. It should be noted that in some regular models and all irregular models, the spectral dynamic analysis had been done based on the Iranian Standard No. 2800. Six types of beams with cross-section of plate girder were used including: TW300F150T15 to W550F250T20 (W: height of web, F: width of flange and T: thickness of web and flange based on mm), and seven types of columns with cross-section of square-box were used including BOX200X15 to BOX500X40 (Dimensions were based on mm). In all sections, criteria of seismic compact sections were considered. ST37 was used in order to design structures such that its yield stress and ultimate stress were 2400 kg/cm^2 and 3600 kg/cm^2, respectively, and Poisson's ratio being 0.30. In the case of irregular frames, a variation in the height of the stories was used to vary the stiffness of the frame (the column section was considered the same in the first and second stories). Panel zone modeling, soil–structure interaction and the effects of the infilled frame were disregarded in the design part. The roof was assumed to be rigid. The effects of P–Δ were also considered. In addition to the design based on the strength criterion, the stiffness distribution of the frames at height was such that the maximum relative lateral displacement angle was limited to the allowance values in Iranian Standard No. 2800.

These frames were adjacent to each other in seven groups according to Table 1. Each group included 45 adjacent combinations. In the recent table, R was abbreviation of the regular frame, I(1.3) was abbreviation of irregular frame which its

Table 1. Combination of studied adjacent frames.

	Floor-to-floor pounding			Floor-to-column pounding		
Group1	Group2	Group3	Group4	Group5	Group6	Group7
NH R.NL R	NH I(1.3). NL I(1.3)	NH I(1.6). NL I(1.6)	NH I(1.3). NL R	NH I(1.6).NL R	NH R. NL I(1.3)	NH R.NL I(1.6)

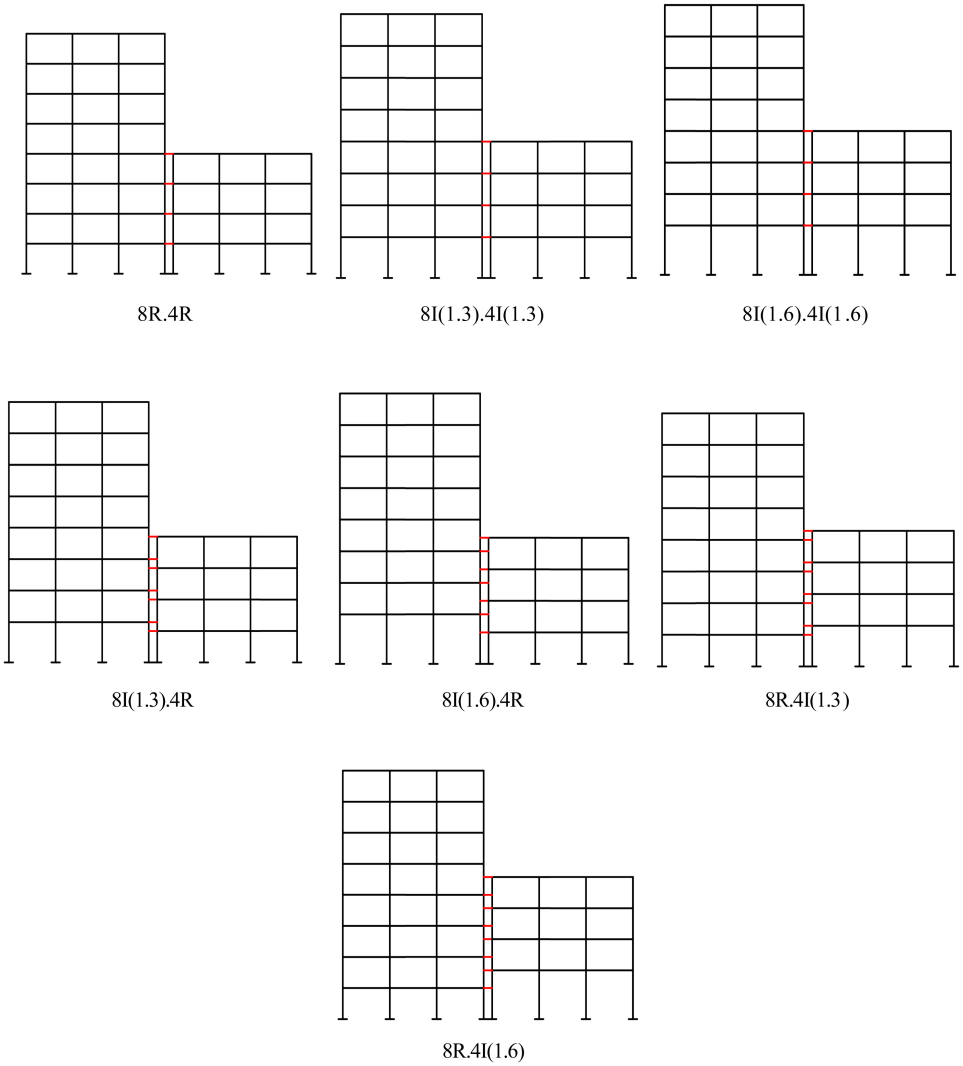

Fig. 1. Adjacent combinations of frames with four and eight stories.

irregular factor was 1.3 (ratio of the height of the first story (4.5 m) to the height of other stories), I(1.6) was abbreviation of irregular frame which its irregular factor was 1.6 (ratio of the height of the first story (5.5 m) to the height of the other stories), N_H and N_L, respectively, denoted the number of taller and shorter frame stories in each investigated combination, which could range from 2 to 20.

In addition to the adjacent combinations of Table 1, 20 adjacent combinations of frames were also investigated which had equal story number of groups 4 and 5 (e.g. 2I(1.3).2R and 2I(1.6).2R). Thus, a total of 335 adjacent combinations had been investigated. In Fig. 1, various adjacent combinations according to Table 1 are shown for adjacency of frames, which had four and eight stories. As can be seen, combinations of groups 1 to 3 showed a floor-to-floor pounding of the adjacent stories and the combinations of groups 4 to 7 showed a floor-to-column pounding of the adjacent stories.

The OPENSEES software was used to do all the nonlinear dynamic analysis of time history. The capabilities of this software were nonlinear dynamics analysis of time history with high reliability [McKenna and Fenves, 2007]. Beams were modeled as displacement-based fiber elements. Each fiber was assumed to exhibit uniaxial bilinear elastoplastic stress–strain cyclic behavior. The behavioral model of the material was type Steel01 with the slope of the hardening area of 0.03. Cycle depreciation was ignored. Panel zones were considered to be rigid and elastic. Force-based fiber elements were used to model the columns to capture moment-axial force interaction effects accurately. Moreover, to account for the axial rigidity of the composite slab, a rigid diaphragm constraint was imposed at the nodes of each floor. Then, in order to account for the P–Δ effects of the gravity loads acting in the tributary plan area of the steel MRF, the Corotational Coordinate Transformation was included in the models. To integrate the equations of motion of the steel MRFs subjected to earthquake ground motion, the Newmark method with constant acceleration was used. The inherent damping ratio of 5% at the first two modes of vibration modeled by using a Rayleigh damping matrix that excluded from its stiffness proportional component in all the nonlinear springs with high initial stiffness so that large damping forces could be avoided.

3. Seismic Sequences

According to available information, sequential earthquakes have occurred in most of the world seismic areas, but unfortunately recorded accelerograms in this kind of natural phenomenon were limited and the main earthquake was only noted in most cases due to differences in the occurrence time of the aftershock and also the less relative magnitude of aftershocks compared to main earthquakes [Abdelnaby, 2012; Mantawy, 2014].

In order to perform nonlinear dynamic analysis, a collection of seven actual recorded seismic sequences was used. The near-fault mainshock record was with progressive directivity effects. Investigations done by Khatami *et al.* [Available Online from 19 March 2020] showed that the average demand of the separation gap of adjacent combinations of regular frames (group 1 of Table 1) at the

highest collision level under near-fault earthquakes was 1.48 times more than that of under far-field earthquakes. The aftershocks were natural and belonged to the same main earthquake record. The aftershocks had been attempted to be selected from the main earthquake recording station. The records were selected from the Pacific Earthquake Engineering Research Center [PEER, 2018], which were studied on soil with type III. One of the main criteria in selecting accelerograms was that the time period of the dominant pulse of their speed was in the range of the fundamental period of the studied frames in this research. Meanwhile, doing sensitivity analysis in order to select the time step, a time step of 0.005 s was used for all the selected records. The earthquake records were applied uniformly to the models and the effects of variations of the distance from the source were not considered. The characteristics of these records are presented in Table 2. Due to the contingency of more than one aftershock, the investigation of the response of the structure was considered under the influence of multiple aftershocks, but it was ignored due to the considerable increase in the time of analysis in this study.

With regards to the aftershock occurrences with intervals ranging from a few seconds to several months after the main earthquake, and in order to conserve the

Table 2. Specifications of earthquake records used in seismic sequences.

No.	Earthquake name	Date (Time)	Station	PGA (g)	Mw	R (km)	Tp (s)	Field & shock type
1–1	Mammoth	1980/05/25 (16:34)	Mammoth Lakes H. S.	0.32	6.1	4.67	0.78	N.M
1–2	Lakes	1980/05/25 (16:49)	Mammoth Lakes H. S.	0.44	5.7	9.12	0.44	N.A
1–3		1980/05/25 (19:44)	Benton	0.18	5.9	44.2	0.40	F.A
2–1	Imperial	1979/10/15 (23:16)	El-Centro Array#4	0.48	6.5	7.05	3.38	N.M
2–2	Valley	1979/10/15 (23:19)	El-Centro Array#4	0.23	5	12.11	0.38	N.A
2–3		1979/10/15 (23:19)	El-Centro Array#2	0.15	5	27.87	0.45	F.A
3–1	Chi-Chi	1999/09/20 (09:20)	CHY101	0.40	7.6	9.94	1.80	N.M
3–2	Taiwan	1999/09/20 (21:46)	TCU079	0.34	6.2	8.48	0.75	N.A
3–3		1999/09/25 (23:52)	CHY101	0.15	6.3	35.97	0.86	F.A
4–1	Northridge	1994/01/17 (12:31)	Jensen Filter Plant	0.62	6.7	5.43	2.10	N.M
4–2		1994/03/20 (21:20)	Jensen Filter Plant	0.26	5.3	14.69	0.40	N.A
4–3		1994/03/20 (21:20)	Santa Monica City Hall	0.10	5.3	24.02	0.33	F.A
5–1	Whittier	1987/10/01 (14:42)	El Monte-Fairview Av	0.25	6	15.67	0.96	N.M

Table 2. (*Continued*)

No.	Earthquake name	Date (Time)	Station	PGA (g)	Mw	R (km)	Tp (s)	Field & shock type
5–2	Narrows	1987/10/04 (10:59)	El Monte-Fairview Av	0.19	5.3	13.28	0.32	N.A
5–3		1987/10/04 (10:59)	Inglewood-Union Oil	0.14	5.3	25.72	0.24	F.A
6–1	Coalinga	1983/05/02 (23:42)	Pleasant Valley P.P.-yard	0.60	6.4	8.41	1.02	N.M
6–2		1983/07/22 (02:39)	Pleasant Valley P.P.-yard	0.58	5.8	13.16	0.42	N.A
6–3		1983/05/09 (02:49)	YUB (temp)	0.33	5.1	28.03	0.36	F.A
7–1	Chalfant Valley	1986/07/20 (14:29)	Zack Brothers Ranch	0.45	6.2	7.58	0.82	N.M
7–2		1986/07/21 (14:42)	Zack Brothers Ranch	0.17	5.7	13.97	0.42	N.A
7–3		1986/07/21 (14:42)	Bishop-LADWP South	0.22	5.7	24.41	0.46	F.A

Notes: PGA: Peak Ground Acceleration; Mw: Moment Magnitude; R: Closest distance from the recording site to the ruptured area; Tp: Predominant Period; N.M: Near-fault. Mainshock; N.A: Near-fault. Aftershock; F.A: Far-field. Aftershock.

time of nonlinear analysis of time history, the structure was subjected to zero acceleration for 50 s after the main earthquake. Investigations showed that the time of 50 s of the structure analysis under zero-acceleration was a suitable time to return the structure to static mode (the end of the vibration under the mainshock). Scaling the near-fault mainshock records was based on the Iranian Standard No. 2800 and the alignment process of accelerograms had been done with Seismosignal software [2016]. The average response spectrum of the elastic acceleration with a damping rate of 5% regarding main earthquakes used in this research is shown in Fig. 2. The scale factors had been extracted 0.65 to 0.80 in the range of the time period of the studied frames.

In order to the more realistic investigation of the effect of sequential earthquakes on the performance of structures and simulations of aftershocks with different intensities compared to the main earthquakes, it was suggested in [Zhai *et al.*, 2014; Garcia *et al.*, 2014; Zhai *et al.*, 2013] that the maximum acceleration of the aftershock should be scaled relative to the maximum acceleration of the main earthquake with different proportions. In this paper, the scale factors of 0.5, 1, 1.5 and 2 had been used to consider the appropriate amplitudes of different aftershock intensities compared to main earthquakes. The possibility of aftershock occurrence with a maximum acceleration which was more than the acceleration of the main earthquake was not far from reality. This aftershock property was not contradictory with the definition nature of the mainshocks and aftershocks. According to Table 2, in some cases, despite the further acceleration of the aftershock, the magnitude of the aftershock was smaller than the main earthquake.

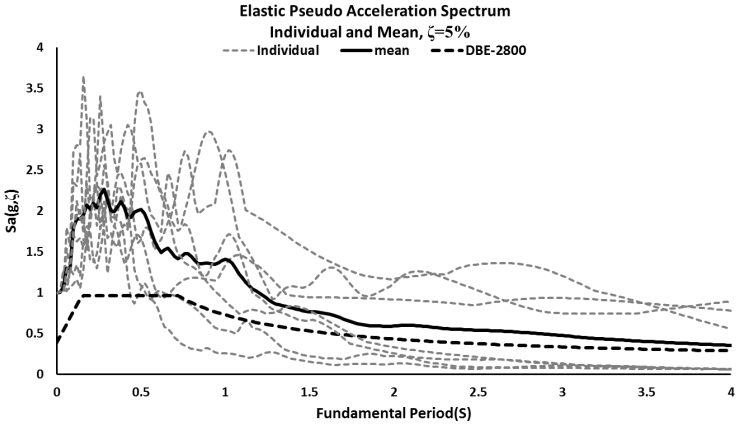

Fig. 2. Elastic acceleration response spectrum for 5% damping corresponding to the investigated near-fault mainshock.

Table 3. Different states in seismic sequence.

No.	Seismic sequence	No.	Seismic sequence
1	N.M + 0.5N.A	9	N.M + 1.5N.A
2	N.M + 0.5F.A	10	N.M + 1.5F.A
3	N.M − 0.5N.A	11	N.M − 1.5N.A
4	N.M − 0.5F.A	12	N.M − 1.5F.A
5	N.M + 1.0N.A	13	N.M + 2.0N.A
6	N.M + 1.0F.A	14	N.M + 2.0F.A
7	N.M − 1.0N.A	15	N.M − 2.0N.A
8	N.M − 1.0F.A	16	N.M − 2.0F.A

Seven singular seismic records were applied to adjacent combinations. In addition, seismic sequences for each of the earthquakes of Table 2 applied in the form of Table 3. Each seismic sequence included the near-fault mainshock, which was once applied to the structures along with the far-field aftershock and once again applied to the structures along with the near-fault aftershock in the form of an artificial seismic sequence. The scale factors were based on PGA_{after}/PGA_{main} and were applied to the 4 levels of 0.5, 1, 1.5 and 2. According to the recommendation of [Efraimiadou *et al.*, 2013b], the effects of changing direction in applying the aftershock record compared to the mainshock were also considered in the studies. In other words, aftershocks were applied to adjacent combinations in two states of opposite direction and the same direction of the mainshock. Generally, 112 artificial seismic sequences according to Table 3 were applied to adjacent combinations.

4. Modeling of Pounding Element

The pounding of adjacent structures naturally occurred when the relative lateral displacement of the adjacent buildings became more than the amount of the

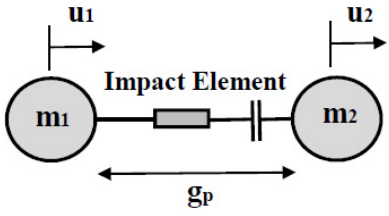

Fig. 3. Pounding element between two masses in collision level.

predicted separation gap due to incorrect estimation or lack of the separation gap. In this case, irreparable damages would be imposed on the structure. In order to model the pounding element in dynamic analysis of time history, in the case of the floor-to-floor pounding of structures adjacent to each other, a model of nonlinear viscoelastic element proposed by Jankowski had been used. According to experimental studies, this element had a higher accuracy than the other proposed elements in the estimation of pounding force. In accordance with Fig. 3, the way of calculating the pounding force of this element was as follows [Jankowski, 2005]:

$$\begin{aligned} F(t) &= \beta.\delta^{\frac{3}{2}}(t) + c(t).\dot{\delta}(t), && \text{if } \delta(t) > 0, \dot{\delta}(t) > 0, \\ F(t) &= \beta.\delta^{\frac{3}{2}}(t), && \text{if } \delta(t) > 0, \dot{\delta}(t) \leq 0, \\ F(t) &= 0, && \text{if } \delta(t) \leq 0, \end{aligned} \tag{1}$$

$$\begin{aligned} \delta(t) &= u_1 - u_2 - g_p, \\ \dot{\delta}(t) &= \dot{u}_1 - \dot{u}_2. \end{aligned} \tag{2}$$

In these relationships, u_1 and u_2 were the lateral displacements of two adjacent structures and g_p was the amount of the separation gap of two adjacent structures. The force in each pounding was calculated based on the relative lateral displacement and relative velocity of the stories. In the recent relationship, β was the stiffness of the pounding element and its calculation was as follows:

$$\beta = \frac{4}{3\pi(h_1 + h_2)} \sqrt{\frac{R_1 \cdot R_2}{R_1 + R_2}}, \tag{3}$$

$$R_i = \sqrt{\frac{3m_i}{4\pi\rho_i}}, \tag{4}$$

$$h_i = \frac{1 - \gamma_i^2}{\pi \cdot E_i}. \tag{5}$$

In these relations $\rho_i, E_i, \gamma_i, m_i, R_i$ were density, elastic modulus, Poisson coefficient, mass and radius equivalent to the pounding objects (the floors), respectively. In this relationship, the steel specifications of ST37 are used with the density of $7850\,\text{kg/m}^3$, the elastic modulus of $2.1 \times 10^6\,\text{kg/cm}^2$ and the Poisson factor of 0.3.

In Eq. (1), the damping parameter $c(t)$ of the pounding element was calculated based on the following equation:

$$c(t) = 2\xi\sqrt{\beta \cdot \sqrt{\delta(t)} \cdot \frac{m_1 \cdot m_2}{m_1 + m_2}}, \tag{6}$$

$$\xi = \frac{9\sqrt{5}}{2} \cdot \frac{1 - e^2}{e(e(9\pi - 16) + 16)}. \tag{7}$$

In the recent relationship, $0 \leq e \leq 1$ was the compensation coefficient. According to the experimental studies carried out by Jankowski for steel-to-steel pounding based on the relative velocity before the pounding, e was calculated as follows:

$$e = -0.0039\ v^3 + 0.0044\ v^2 - 0.1867v + 0.7299. \tag{8}$$

The behavior of the nonlinear viscoelastic pounding element was coded as a new material in programming language VC ++ according to the conditional equation (1) and was used with the help of the modeling interface of the program in OPENSEES software. In this code, all of the effective parameters in the calculation of force (such as compensation coefficient, damping, and stiffness of the pounding element in each cycle of poundings) were updated based on the displacement and velocity of the pounding points.

5. Modeling Accuracy Verification

In order to verify the modeling of the steel moment frame under a nonlinear analysis, the four-story frame of [Garcia and Negrete-Manriquez, 2011] was used. The geometric specifications and cross-section of elements of this frame (with office usage) are shown in Fig. 4(a).

It should be mentioned that the frame had uniform mass distribution and a non-uniform lateral stiffness distribution was applied over the height. A bilinear moment–curvature relationship, that its strain-hardening ratio was equal to 2%, was considered to model the behavior of the steel columns and beams. The flexural moment capacity for beams and columns was determined using the actual yield strength capacity of 337.8 MPa and 399.9 MPa, respectively. Rayleigh damping, which was equal to 5% of critical damping, was assigned to the first and second modes for the four-story frame [Garcia and Negrete-Manriquez, 2011]. This frame was analyzed under near-fault earthquake record of Northridge (Rinaldi Receiving Sta) in OPENSEES software. The time history of the lateral displacement of the first floor in the analytical model and model [Garcia and Negrete-Manriquez, 2011] are presented in Figs. 4(b) and 4(c), which had acceptable compliance in terms of the form and the maximum lateral displacement.

In order to verify the accuracy of the used modeling in the floor-to-floor pounding of adjacent buildings, an experimental model of [Takabatake *et al.*, 2014] was

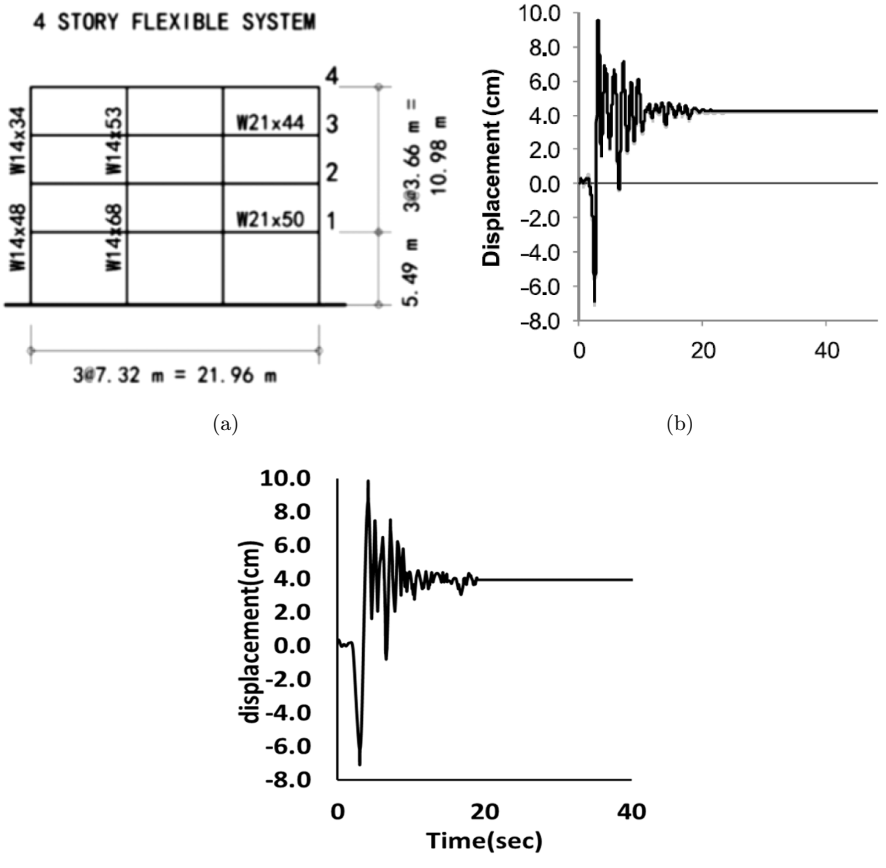

Fig. 4. (a) Elevation of four-story steel frame [Garcia and Negrete-Manriquez, 2011]. (b) Time history of lateral displacement in [Garcia and Negrete-Manriquez, 2011]. (c) Time history of lateral displacement in an analytical model.

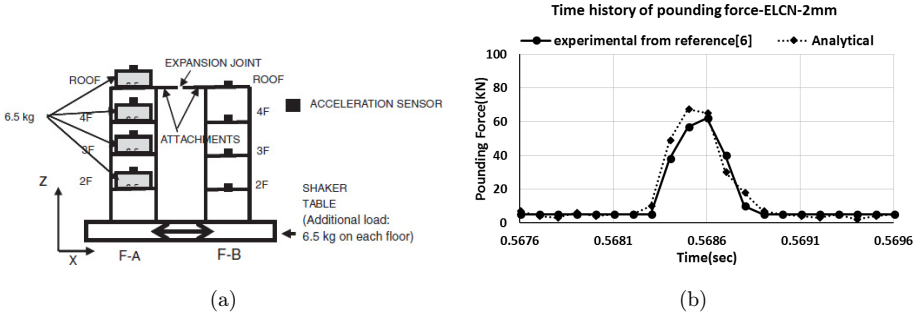

Fig. 5. (a) Experimental sample details of the pounding of adjacent frames on a shaking table [Takabatake *et al.*, 2014]. (b) Time history of the pounding forces of analytical and experimental models.

modeled in OPENSEES, which had two frames with single span and four-story with the specification in Fig. 5(a). This model was placed in the laboratory on a one-directional shaking table. The span, depth, and height of the frames were 0.2, 0.15 and 0.6 m, respectively. The height of all stories was the same and was equal to 0.15 m. In the frame F-A, there was an additional mass of 6.5 kg in all stories. The samples had no beam and the floor of the frames was made up of aluminum rectangular plates with dimensions of $0.15\,\text{m} \times 0.2\,\text{m} \times 0.015\,\text{m}$. The separation gap length was considered at 2 mm at the highest level between the two frames. Accelerogram of the EL-Centro 1940 NS was applied to the frame at a normalized maximum velocity of 0.5 m/s by using the shaking table.

The analytical model in the software was considered as two frames with four-degree-of-freedom and concentrated mass in the roof level in accordance with the mass distributions in [Takabatake *et al.*, 2014]. The fixed damping coefficient for each frame was considered as 0.02. For modeling of pounding element, a nonlinear viscoelastic pounding element model was proposed by Jankowski. The compensation coefficient was assumed as 0.63, and the related results of the experimental pounding force and analytical pounding force were compared under the ELCN record based on the separation gap of 2 mm. Figure 5(b) provids acceptable consistency in terms of the form of variation and the maximum pounding force at the highest level. In this figure, the maximum pounding forces of the experimental and analytical model for the separation gap of 2 mm were 61.48 KN and 67.30 KN, respectively.

6. Results of Time History Dynamic Analysis

In this section, the results of the time history dynamic analysis were presented regarding the demand for separation gap of adjacent frames under the seismic sequence effects. The important point was the irregularity effect of the lateral stiffness (in the form of soft-story in the first story of the frames) on the separation gap of the two adjacent structures. The non-dimensional parameter of the NSG was obtained by dividing the demand separation gap into the height of the highest collision level of two frames from the base.

For example, in Fig. 6, the time history of lateral displacement and the separation gap of the adjacent combination of 8R.4R are shown at the highest collision level. In this figure, the time history of the separation gap demand with the purpose of preventing the pounding of two structures had been extracted from the investigation of six possible states based on the difference in the dynamic lateral displacement of the adjacent moment frames during the analysis period. Seismic sequences No. 9 and 11 of Table 3 from the Northridge earthquake were applied to this adjacent combination. These seismic sequences were a combination of records of 4–1 and 4–2 in Table 2 (the near-fault mainshock and the near-fault aftershock) with $\text{PGA}_{\text{after}}/\text{PGA}_{\text{main}} = 1.50$. As can be seen, due to the effect of applying the mainshock along with the aftershock, the amount of separation gap demand to prevent poundings of these two structures increased from 16.2 cm to 20.2 cm. Also, due to the

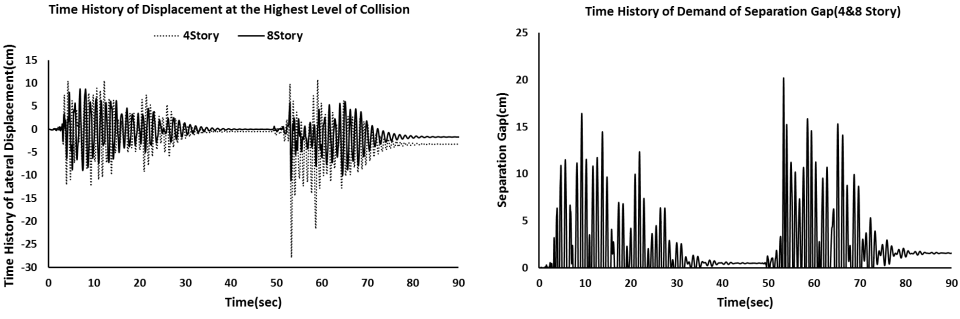

(a) (b)

Fig. 6. Time history of lateral displacement and separation gap of the combination of 8R.4R under the seismic sequence of the Northridge earthquake.

effect of applying aftershock after the mainshock and the development of doubled residual deformations of two structures, the amount of the residual separation gap after analyzing increased approximately three times in comparison with the state of applying the singular mainshock.

Presented results in the following are based on the average of the NSG and the average of an incremental factor of the NSG in the seismic sequence in comparison with applying the singular earthquake resulting from the dynamic analysis of the time history under the investigated earthquake records.

Table 4. Average of NSG for all adjacent combinations under mainshock seismic records of Table 2.

				NSG			NSG			NSG	
No.	Group1	NSG	Groups 2&3	I(1.3)	I(1.6)	Groups 4&5	I(1.3)	I(1.6)	Groups 6&7	I(1.3)	I(1.6)
1	4R.2R	0.006	4I.2I	0.008	0.010	4I.2R	0.011	0.017	4R.2I	0.008	0.012
2	6R.2R	0.011	6I.2I	0.013	0.021	6I.2R	0.015	0.030	6R.2I	0.012	0.014
3	6R.4R	0.009	6I.4I	0.011	0.015	6I.4R	0.014	0.025	6R.4I	0.007	0.012
4	8R.2R	0.014	8I.2I	0.015	0.017	8I.2R	0.018	0.020	8R.2I	0.012	0.013
5	8R.4R	0.013	8I.4I	0.014	0.017	8I.4R	0.017	0.022	8R.4I	0.010	0.012
6	8R.6R	0.007	8I.6I	0.008	0.010	8I.6R	0.011	0.015	8R.6I	0.006	0.011
7	10R.2R	0.021	10I.2I	0.024	0.031	10I.2R	0.024	0.034	10R.2I	0.021	0.022
8	10R.4R	0.015	10I.4I	0.019	0.020	10I.4R	0.020	0.027	10R.4I	0.013	0.016
9	10R.6R	0.012	10I.6I	0.012	0.013	10I.6R	0.015	0.020	10R.6I	0.010	0.013
10	10R.8R	0.007	10I.8I	0.009	0.010	10I.8R	0.011	0.015	10R.8I	0.007	0.010
11	12R.2R	0.020	12I.2I	0.023	0.028	12I.2R	0.022	0.028	12R.2I	0.019	0.022
12	12R.4R	0.016	12I.4I	0.020	0.023	12I.4R	0.021	0.027	12R.4I	0.018	0.020
13	12R.6R	0.015	12I.6I	0.016	0.018	12I.6R	0.019	0.023	12R.6I	0.014	0.016
14	12R.8R	0.011	12I.8I	0.013	0.014	12I.8R	0.013	0.017	12R.8I	0.012	0.014
15	12R.10R	0.007	12I.10I	0.007	0.009	12I.10R	0.010	0.013	12R.10I	0.006	0.007
16	14R.2R	0.020	14I.2I	0.027	0.037	14I.2R	0.024	0.036	14R.2I	0.022	0.024
17	14R.4R	0.018	14I.4I	0.023	0.027	14I.4R	0.023	0.031	14R.4I	0.020	0.021
18	14R.6R	0.017	14I.6I	0.019	0.020	14I.6R	0.022	0.026	14R.6I	0.017	0.018
19	14R.8R	0.014	14I.8I	0.017	0.018	14I.8R	0.018	0.022	14R.8I	0.015	0.017
20	14R.10R	0.011	14I.10I	0.012	0.014	14I.10R	0.014	0.017	14R.10I	0.010	0.013

Table 4. (*Continued*)

				NSG			NSG			NSG	
No.	Group1	NSG	Groups 2&3	I(1.3)	I(1.6)	Groups 4&5	I(1.3)	I(1.6)	Groups 6&7	I(1.3)	I(1.6)
21	14R.12R	0.007	14I.12I	0.008	0.009	14I.12R	0.010	0.014	14R.12I	0.007	0.008
22	16R.2R	0.019	16I.2I	0.026	0.033	16I.2R	0.023	0.031	16R.2I	0.022	0.025
23	16R.4R	0.019	16I.4I	0.024	0.030	16I.4R	0.025	0.031	16R.4I	0.022	0.023
24	16R.6R	0.018	16I.6I	0.020	0.022	16I.6R	0.022	0.027	16R.6I	0.019	0.020
25	16R.8R	0.017	16I.8I	0.020	0.021	16I.8R	0.021	0.024	16R.8I	0.019	0.019
26	16R.10R	0.014	16I.10I	0.015	0.017	16I.10R	0.016	0.020	16R.10I	0.014	0.016
27	16R.12R	0.011	16I.12I	0.012	0.013	16I.12R	0.014	0.017	16R.12I	0.011	0.011
28	16R.14R	0.006	16I.14I	0.006	0.007	16I.14R	0.008	0.011	16R.14I	0.006	0.006
29	18R.2R	0.020	18I.2I	0.030	0.039	18I.2R	0.028	0.038	18R.2I	0.025	0.028
30	18R.4R	0.021	18I.4I	0.027	0.033	18I.4R	0.027	0.035	18R.4I	0.024	0.026
31	18R.6R	0.020	18I.6I	0.023	0.025	18I.6R	0.025	0.030	18R.6I	0.021	0.023
32	18R.8R	0.018	18I.8I	0.021	0.023	18I.8R	0.022	0.026	18R.8I	0.020	0.021
33	18R.10R	0.016	18I.10I	0.018	0.019	18I.10R	0.019	0.022	18R.10I	0.017	0.018
34	18R.12R	0.013	18I.12I	0.015	0.016	18I.12R	0.016	0.019	18R.12I	0.014	0.014
35	18R.14R	0.010	18I.14I	0.011	0.012	18I.14R	0.013	0.016	18R.14I	0.010	0.011
36	18R.16R	0.005	18I.16I	0.006	0.007	18I.16R	0.008	0.011	18R.16I	0.005	0.006
37	20R.2R	0.023	20I.2I	0.034	0.044	20I.2R	0.032	0.043	20R.2I	0.029	0.032
38	20R.4R	0.024	20I.4I	0.031	0.038	20I.4R	0.032	0.041	20R.4I	0.028	0.030
39	20R.6R	0.023	20I.6I	0.026	0.029	20I.6R	0.029	0.035	20R.6I	0.024	0.025
40	20R.8R	0.020	20I.8I	0.024	0.026	20I.8R	0.024	0.028	20R.8I	0.023	0.024
41	20R.10R	0.018	20I.10I	0.020	0.022	20I.10R	0.022	0.025	20R.10I	0.019	0.020
42	20R.12R	0.015	20I.12I	0.017	0.019	20I.12R	0.018	0.021	20R.12I	0.016	0.017
43	20R.14R	0.013	20I.14I	0.015	0.016	20I.14R	0.016	0.019	20R.14I	0.014	0.015
44	20R.16R	0.010	20I.16I	0.012	0.014	20I.16R	0.013	0.016	20R.16I	0.011	0.011
45	20R.18R	0.007	20I.18I	0.008	0.009	20I.18R	0.010	0.013	20R.18I	0.007	0.008
46	—	—	—	—	—	2I.2R	0.010	0.019	—	—	—
47	—	—	—	—	—	4I.4R	0.008	0.017	—	—	—
48	—	—	—	—	—	6I.6R	0.007	0.016	—	—	—
49	—	—	—	—	—	8I.8R	0.005	0.010	—	—	—
50	—	—	—	—	—	10I.10R	0.005	0.010	—	—	—
51	—	—	—	—	—	12I.12R	0.003	0.008	—	—	—
52	—	—	—	—	—	14I.14R	0.003	0.007	—	—	—
53	—	—	—	—	—	16I.16R	0.002	0.005	—	—	—
54	—	—	—	—	—	18I.18R	0.002	0.006	—	—	—
55	—	—	—	—	—	20I.20R	0.002	0.006	—	—	—

The average of NSG at the highest collision level for the 335 investigated adjacent combinations under the mainshock (singular) seismic records from Table 2 are shown in Table 4. The NSG in the seismic sequence was compared with the values in Table 4 and the incremental factors of the NSG were presented. It should be noted in this table that the study of adjacent combinations with frames was discarded having equal stories in groups 1, 2 and 3 (e.g. 4R.4R or 4I(1.3).4I(1.3) or 4I(1.6).4I(1.6)). The separation gap obtained from the analysis was zero in these adjacent combinations due to the same dynamic properties of the two adjacent frames. Also, in groups 6 and 7, the adjacent combinations of the frames with equal stories were similar to rows 46–55 in groups 4 and 5 of Table 4, which were not repeated.

6.1. *Determination of critical seismic sequence*

With regards to different states in applying mainshock–aftershock to adjacent combinations, choosing the most critical state in order to increase the separation gap had significant importance compared to the state of applying the singular earthquake. For this purpose, Fig. 7 shows the incremental factor of the NSG in the combination of two frames with four and eight-story among all adjacent groups of Table 1. Figures 7(a) and 7(b), respectively, are related to seismic sequences with near-fault and far-field aftershocks under different ratios of PGA_{after}/PGA_{main}.

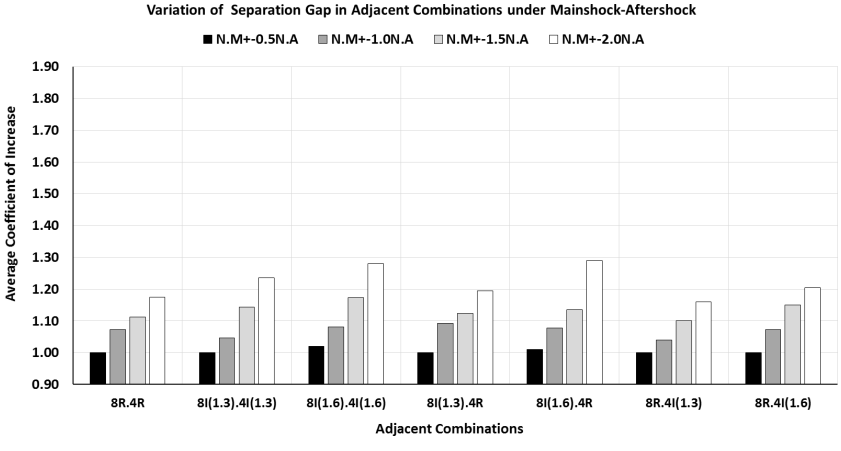

(a)

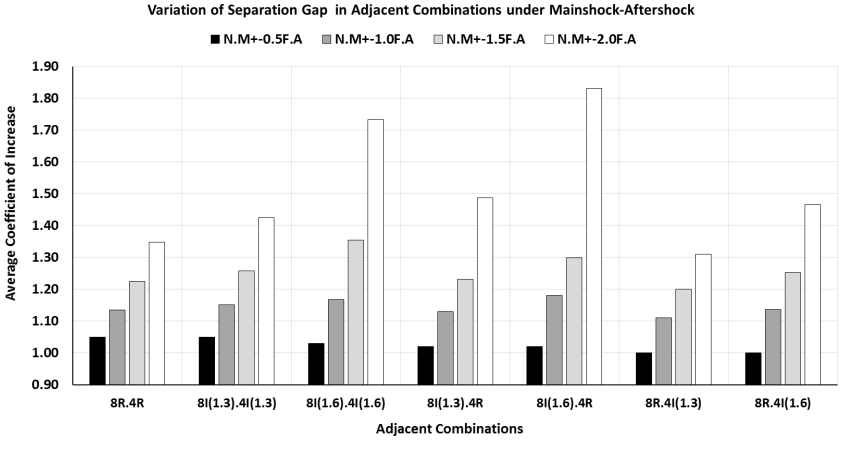

(b)

Fig. 7. The incremental factors of the NSG in the combination of two frames with four and eight-story among all investigated adjacent groups. (a) The incremental factor of the NSG under the near-fault mainshock and the near-fault aftershock. (b) The incremental factor of the NSG under the near-fault mainshock and the far-field aftershock.

It should be noted that according to the recommendation of [Efraimiadou *et al.*, 2013b], the states related to the changing direction of the aftershock record compared to the mainshock were investigated. Therefore, the maximum amount of the incremental factor of the NSG of two states was considered as the action criterion. The results showed that the incremental factor of the NSG in seismic sequence in the form of the near-fault mainshock and the far-field aftershock was more than the state of applying the near-fault mainshock and the near-fault aftershock, especially in higher ratios of $\mathrm{PGA}_{\mathrm{after}}/\mathrm{PGA}_{\mathrm{main}}$.

As an example in the combination of 8I(1.6).4R, the incremental factor of the NSG under seismic sequence with the far-field aftershock and by considering $\mathrm{PGA}_{\mathrm{after}}/\mathrm{PGA}_{\mathrm{main}} = 1.50, 2.0$ was 14% and 42% more than the seismic sequence with the near-fault aftershock, respectively. This increase was not so significant in the ratio of $\mathrm{PGA}_{\mathrm{after}}/\mathrm{PGA}_{\mathrm{main}} = 0.50$. In other words, for this ratio, the incremental factor in both Figs. 7(a) and 7(b) was close to 1. Therefore, the seismic sequence in this range had not been able to increase the amount of the NSG compared to the state of applying the singular earthquake. According to results obtained in this section, in the following, results are provided based on applying seismic sequence with the far-field aftershock.

6.2. *Comparison of analytical results and regulations amount regarding the NSG of adjacent structures*

The NSG obtained from the time history dynamic analysis for the adjacent different combinations of regular frames up to eight stories is shown in Fig. 8. According to Iranian Standard No. 2800 for these adjacent combinations which had the same base level, the NSG demand was 0.01 of height of the highest collision level of two frames from the base level. As it can be seen, in some adjacent combinations under a singular

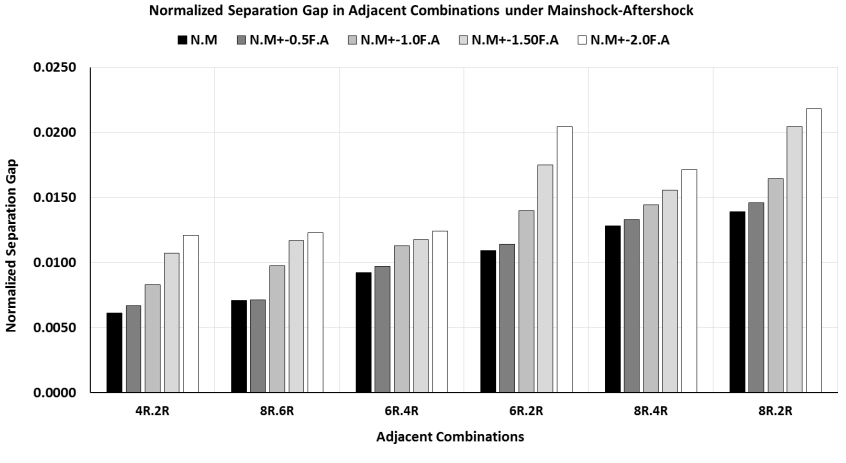

Fig. 8. The NSG of adjacent combinations of frames up to eight-story under the effect of singular and sequential earthquakes.

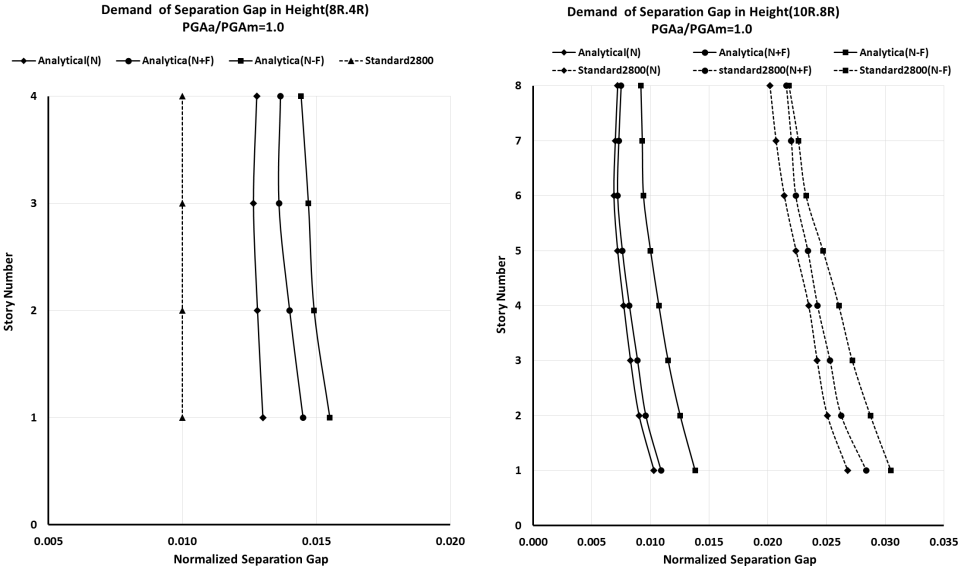

(a) (b)

Fig. 9. Demand variations of the NSG in height under seismic sequence and compared it with criteria of the regulation. (a) The NSG at the collision levels of two frames with four and eight-story. (b) The NSG at the collision levels of two frames with eight and ten-story.

earthquake, the amount of the NSG exceeded the permissible amount of the regulation. This was while in all investigated combinations under seismic sequence, and for $\mathrm{PGA}_{\mathrm{after}}/\mathrm{PGA}_{\mathrm{main}} = 1.50, 2.0$, the amount of the NSG was more than 0.01 and in some cases was more than twice that amount. For example, the NSGs in the adjacent combination of 8R.2R and for $\mathrm{PGA}_{\mathrm{after}}/\mathrm{PGA}_{\mathrm{main}} = 1.50, 2.0$ were equal to 0.0205 and 0.0218, respectively. Therefore, if the seismic sequence happened, in many states, the NSG would be underestimated based on the Iranian Standard No. 2800.

In Fig. 9(a), variations of the NSG at the collision levels of the adjacent combination of 8R.4R are shown and compared with a permissible amount of Standard No. 2800. The results showed that in the state of applying singular and sequential earthquakes, the resulted NSG from the analysis was greater than the permissible amount of the regulation. For example, maximum NSG at the highest collision level of the two frames with four and eight-story under the seismic sequence of N.M-1.0F.A reached about 1.40 times more than the amount of Standard No. 2800. In Fig. 9(b), variations of the NSG at the collision levels of the adjacent combination of 10R.8R indicated that the permissible amounts of Standard No. 2800 (the criteria of section 12.12.3 of the ASCE/SEI 7-16) showed an overestimate of the NSG. So that, average permissible amounts of the regulation at the all collision levels were approximately 2.4 times more than the resulted amounts from analysis under the seismic sequence of N.M-1.0F.A.

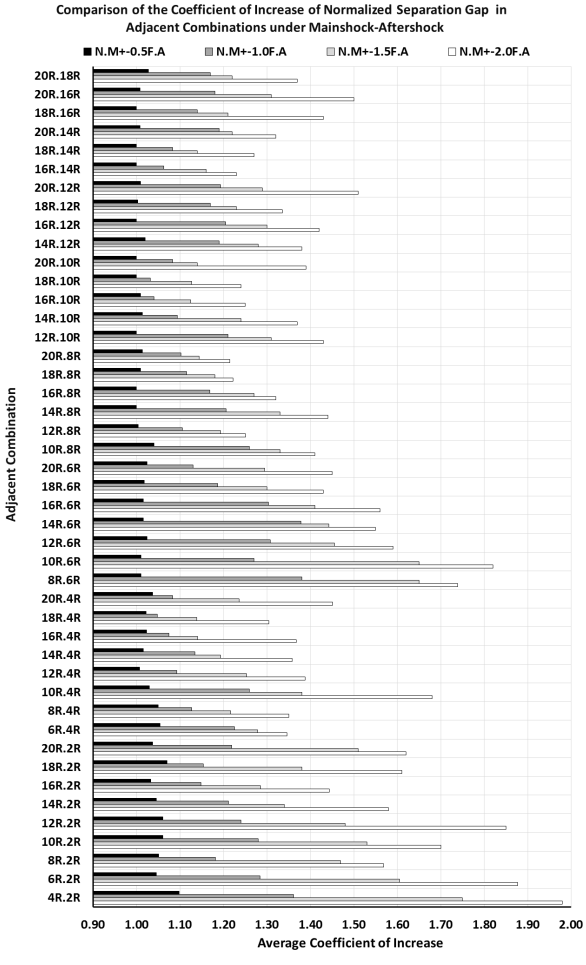

Fig. 10. Seismic sequence effect on the increase of the adjacent combinations separation gap of regular frames.

6.3. *Adjacent combinations of regular structures under the effect of the near-fault mainshock and far-field aftershock*

Figure 10, showed the effect of applying the seismic sequence in the form of near-fault mainshock/far-field aftershock with different ratios of $\mathrm{PGA}_{\mathrm{after}}/\mathrm{PGA}_{\mathrm{main}}$ on all studied adjacent combinations of group 1 based on Table 1. The horizontal axis of this figure represents the incremental factor of the NSG in seismic sequences relative to the state of applying singular earthquake. The results showed that by increasing the ratio $\mathrm{PGA}_{\mathrm{after}}/\mathrm{PGA}_{\mathrm{main}}$, the separation gap amount increased, so that the increased average of the NSG of all investigated combinations under seismic sequence with $\mathrm{PGA}_{\mathrm{after}}/\mathrm{PGA}_{\mathrm{main}} = 1.0, 1.5$ was 1.18 and 1.31 times more than the state of applying the singular earthquake, respectively. The amount of this increase was about two times in some models for ratio $\mathrm{PGA}_{\mathrm{after}}/\mathrm{PGA}_{\mathrm{main}} = 2.0$.

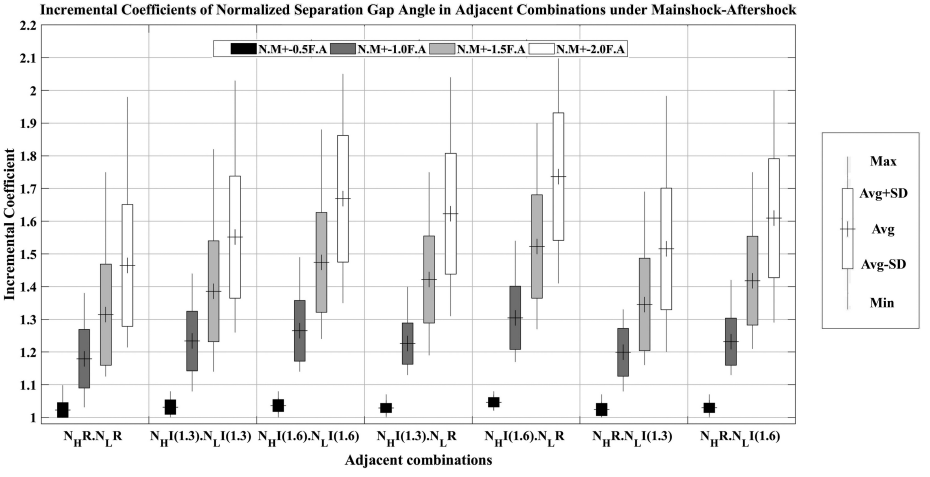

Fig. 11. Seismic sequence effect on incremental factor variations of the separation gap of all regular and irregular adjacent combinations.

6.4. *Effect of the seismic sequence on adjacent combinations of regular and irregular structures*

Due to a large number of models and different seismic sequences, the conclusion of the results of the analysis of all the adjacent combinations of Table 1 is shown in Fig. 11. In this figure, for each group of adjacent combinations, the average amount, maximum and minimum amount, and standard deviation amount of the incremental factor of the NSG in the seismic sequence were given.

The results showed that by developing and increasing the irregular amount of the lateral stiffness of the first story of the adjacent combinations, the incremental factor of the NSG increased compared to the regular basis combinations (NH R.NL R). This increase in the seismic sequence was not significant when $PGA_{after}/PGA_{main} = 0.50$, but with the increasing ratio of PGA_{after}/PGA_{main}, the amount of the incremental factor increased. As an example, when $PGA_{after}/PGA_{main} = 1.50$ in group combinations of NH I(1.3).NL I(1.3) and NH I(1.6).NL I(1.6), the average incremental factors were 1.39 and 1.47, respectively. These amounts were more than the average incremental factor of 1.31 belonging to group combinations of NH R.NL R, because in the irregular frames, due to increasing the lateral displacement caused by the existence of soft story and exacerbating it by applying aftershocks after the mainshock, the NSG increased to a greater extent.

On the other hand, in the ratio of $PGA_{after}/PGA_{main} = 1.50$ for the group combinations of NH I(1.6).NL R, the average incremental factor of the NSG reached 1.52. However, this factor was 1.47 and 1.42 for group combinations of NH I(1.6).NL I(1.6) and NH R.NL I(1.6). Therefore, the development of a soft story in the taller frame of adjacent combinations had a greater increase in the separation gap amount under seismic sequence relative to the state of the development of the soft story in both

adjacent frames (with the same lateral stiffness irregularities). The incremental factor in the latter state was more than the incremental factor of the separation gap in irregular adjacent combinations with a soft story in the shorter frame.

The maximum incremental factor of the separation gap based on already done analyses was 2.12, which belonged to group combinations of NHI(1.6).NLR with a ratio of $PGA_{after}/PGA_{main} = 2.0$. Therefore, applying an aftershock with greater intensity than the main earthquake, along with the development of lateral stiffness irregularity in the form of soft-story in the adjacent combination, could increase the separation gap demand by more than 2 times.

The results of the done analysis on the effects of the seismic sequence (the near-fault mainshock and the far-field aftershock) on the NSG of all investigated adjacent combinations are shown in Fig. 12. As an example, while $PGA_{after}/PGA_{main} = 1.0$, in 37% of the adjacent combinations, the increased amount of the NSG was more than 20% compared to the state of applying singular earthquake. However, by increasing PGA_{after}/PGA_{main} into 1.50, 48% of adjacent combinations experienced an increase in the NSG which was more than 35%. The effects of seismic sequence except in ratio of $PGA_{after}/PGA_{main} = 0.50$, that in 88% of the adjacent combinations caused an increase of less than 5% in the NSG, was significant. Therefore, these effects would be considered in the process of determining the NSG, especially in prone areas to the occurrence of seismic sequence.

6.5. *Proposing a relationship regarding the effect of the seismic sequence on the separation gap of adjacent structures and validation of the proposed relationship*

The following relation was proposed based on the results obtained from the analysis and the selection of effective parameters such as the ratio of the aftershock intensity

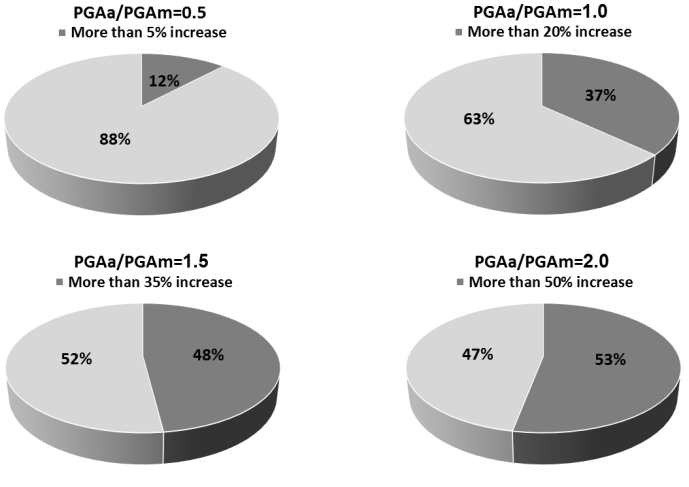

Fig. 12. The effect of seismic sequence on increasing the separation gap amount of all regular and irregular adjacent combinations.

to the mainshock intensity, and the ratio of the lateral stiffness of the first story of the adjacent frames to the lateral stiffness of the other stories. This relationship was presented by selecting the appropriate objective function with the help of nonlinear regression and based on the average of the minimum percentage error between analytic and estimated values. The recent relationship, in the form of a factor which was more than 1, showed seismic sequence effects on the estimated separation gap of the adjacent combinations of regular and irregular frames with the soft-story, and consisted of three separate sections. The first term was about seismic sequence effect that was shown as the ratio of the maximum acceleration of the aftershock to the maximum acceleration of the mainshock. This ratio was related to the studied critical seismic sequence (the near-fault mainshock and the far-field aftershock). The second and third terms represented the irregular effects of the lateral stiffness in the form of the soft story in the first story of the adjacent frames. As it was clear from the relationship, the increase in the height of the first story in the taller frame of the adjacent combinations had a greater effect on the incremental factor of the separation gap.

$$\alpha_{\mathrm{ME}} = 1 + 0.15\left(\frac{\mathrm{PGA}_{\mathrm{after}}}{\mathrm{PGA}_{\mathrm{main}}}\right)^{1.8}\left(\frac{h_H^*}{h_0}\right)^{0.7}\left(\frac{h_L^*}{h_0}\right)^{0.15}. \tag{9}$$

In this relationship, α_{ME} was the incremental factor of the NSG caused by the seismic sequence effect, $\mathrm{PGA}_{\mathrm{after}}, \mathrm{PGA}_{\mathrm{main}}$, respectively, were the maximum acceleration of the aftershock and the mainshock, h_L^*, h_H^*, respectively, were the height of the first story of the shorter and taller frames, and h_0 was the height of the other stories of adjacent frames. It should be noted that α_{ME} was 1 in the absence of applying aftershock, and the term regarding irregularity would be effective in determining α_{ME} when the seismic sequence was applied to combinations.

Table 5. Validation of the proposed factor based on the results obtained from the analysis.

Adjacent combination	$\frac{\mathrm{PGA}_{\mathrm{after}}}{\mathrm{PGA}_{\mathrm{main}}}$	$\frac{h_H^*}{h_0}$	$\frac{h_L^*}{h_0}$	Analytical incremental factor	α_{ME}	Ratio of analytical incremental factor to α_{ME}
10R.4R	0.5	1.0	1.0	1.03	1.04	0.99
6I(1.3).2I(1.3)	0.5	1.28	1.28	1.06	1.05	1.01
18I(1.6).8I(1.6)	0.5	1.57	1.57	1.04	1.06	0.98
16I(1.3).14R	1.0	1.28	1.0	1.15	1.18	0.97
16I(1.6).2R	1.0	1.57	1.0	1.28	1.21	1.06
18R.12I(1.3)	1.0	1.0	1.28	1.21	1.16	1.04
14R.2I(1.6)	1.0	1.0	1.57	1.20	1.16	1.03
18R.6R	1.5	1.0	1.0	1.30	1.31	0.99
12I(1.3).6I(1.3)	1.5	1.28	1.28	1.43	1.39	1.03
20I(1.6).14I(1.6)	1.5	1.57	1.57	1.38	1.46	0.95
20I(1.3).8R	1.5	1.28	1.0	1.32	1.37	0.96
8I(1.6).4R	2.0	1.57	1.0	1.83	1.72	1.06
6R.4I(1.3)	2.0	1.0	1.28	1.43	1.54	0.93
10R.8I(1.6)	2.0	1.0	1.57	1.61	1.56	1.03

In other words, only the secondary effects (intensifier) associated with the development of soft story had been seen in the recent relationship due to application of the mainshock along with the aftershock. The average of the absolute error of the analytic and suggested values of Eq. (9) was 0.10.

In order to validate the proposed relationship, the values of the incremental factor in the NSG obtained from the analysis and the proposed Eq. (9) for some adjacent combinations are presented in Table 5. Required parameters for calculating the incremental factor are given in this table. Obtained results showed that the difference, which was less than 10% of the analytical and estimated incremental factors, was reasonable and negligible.

7. Conclusion

This study estimated the incremental factor of the NSG demand at the highest collision level of 335 adjacent combinations of regular and irregular steel moment frames. The results of the done analyses under a set of 119 singular and sequential earthquake records are as follows:

- In the seismic sequence, in the case of the near-fault mainshock and the far-field aftershock, the incremental factor of the NSG relative to the state of applying singular earthquake was more than the seismic sequence in the form of the near-fault mainshock and the near-fault aftershock.
- In most cases of adjacent regular frames with height up to eight stories, the NSG obtained from the analysis under seismic sequence was greater than the 0.01 of recommended in Standard No. 2800, which represented an underestimated amount of the separation gap by regulations. The NSG obtained from Standard No. 2800 (ASCE/SEI 7-16) in the combination of regular frames, which had more than eight stories, was more than analytical amounts. As in the combination of two regular frames of 8 and 10, the amounts of the regulations were, on average, 2.4 times greater than the amounts obtained from the analysis under seismic sequence with the ratio of $\mathrm{PGA}_{\mathrm{after}}/\mathrm{PGA}_{\mathrm{main}} = 1.0$.
- By developing and increasing the amount of irregularities of the lateral stiffness on the first story of adjacent combinations, the incremental factor of the NSG increased compared to the incremental factor of regular basis combinations. Developing a soft story in the taller frame of the adjacent combinations created a greater increase in the separation gap amount under seismic sequence relative to the state of developing a soft story (with a same lateral stiffness irregularity) on both adjacent frames. In addition, the incremental factor in the latter case was more than the incremental factor of the separation gap of adjacent combinations with the soft story in the shorter frame.
- In a seismic sequence with a ratio of $\mathrm{PGA}_{\mathrm{after}}/\mathrm{PGA}_{\mathrm{main}} = 0.50$, among 88% of the adjacent combinations, less than 5% of the increase in the NSG was caused in

comparison with the singular earthquake, so the increase of the NSG in this range was not significant and could be ignored.

- Among the total analyses of seismic sequences with the ratio of $PGA_{after}/PGA_{main} = 1.0, 1.50$, 37% and 48% of the adjacent combinations, the increase of demand for separation gap compared to the state of applying the singular earthquake was more than 20% and 35%, respectively. Therefore, seismic sequence effects were significant and would be considered in the process of determining the NSG, especially in prone areas to the occurrence of seismic sequence.
- On the basis of the analysis, a relationship was proposed with the aim of estimating the incremental factor of the NSG of adjacent structures under seismic sequence by considering the effect of developing soft-story on the lowest story.

References

Abdelnaby, A. E. [2012] "Multiple earthquake effects on degrading reinforced concrete structures," Ph.D. thesis, Civil Engineering Dept., University of Illinois at Urbana-Champaign.

ASCE/SEI 7-16 [2016] "American society of civil engineers," *Minimum Design Loads for Buildings and Other Structures*, USA.

Efraimiadou, S., Hatzigeorgiou, G. D. and Beskos, D. E. [2013a] "Structural pounding between adjacent buildings subjected to strong ground motions. Part I: The effect of different structures arrangement," *Earthq. Eng. Struct. Dyn.* **42**, 1509–1528.

Efraimiadou, S., Hatzigeorgiou, G. D. and Beskos, D. E. [2013b] "Structural pounding between adjacent buildings subjected to strong ground motions. Part II: The effect of multiple earthquakes," *Earthq. Eng. Struct. Dyn.* **42**, 1529–1545.

ETABS [2015] *Analysis Reference Manual (Version 15.2.2)* (Computers and Structures Inc., Berkeley, USA).

Faisal, A., Majid, T. A. and Hatzigeorgiou, G. D. [2013] "Investigation of story ductility demands of inelastic concrete frames subjected to repeated earthquakes," *Soil Dyn. Earthq. Eng.* **44**, 42–53.

Favvata, M. J. [2017] "Minimum required separation gap for adjacent RC frames with potential inter-story seismic pounding," *Eng. Struct.* **152**, 643–659.

Garcia, R. and Negrete-Manriquez, C. [2011] "Evaluation of drift demands in existing steel frames under as-recorded far-field and near-fault mainshock-aftershock seismic sequences," *Eng. Struct.* **33**, 621–634.

Garcia, R. [2012] "Mainshock-Aftershock ground motion features and their influence in buildings seismic response," *J. Earthq. Eng.* **16**, 719–737.

Garcia, R., Marin, M. V. and Gilmore, A. T. [2014] "Effect of seismic sequences in reinforced concrete frame buildings located in soft-soil sites," *Soil Dyn. Earthq. Eng.* **63**, 56–68.

Hao, H. [2015] "Analysis of seismic pounding between adjacent buildings," *Aust. J. Struct. Eng.* **16**(3), 208–225.

Hatzigeorgiou, G. D. and Pnevmatikos, N. G. [2014] "On the seismic response of collided structures," *Int. J. Civil Arch. Struct. Constr. Eng.* **8**(7), 750–754.

Hatzivassiliou, M. and Hatzigeorgiou, G. D. [2015] "Seismic sequence effects on three-dimensional reinforced concrete buildings," *Soil Dyn. Earthq. Eng.* **72**, 77–88.

Hosseinpour, F. and Abdelnaby, A. E. [2017] "Effect of different aspects of multiple earthquakes on the nonlinear behavior of RC structures," *Soil Dyn. Earthq. Eng.* **92**, 706–725.

Iranian National Building Code (INBC)-Division 6 [2014] Road, housing and Urban development research center, *Design Loads for Buildings*, Iran.

Iranian National Building Code (INBC)-Division 10 [2014] Road, housing and Urban development research center, *Design and Construction of Steel Structures*, Iran.

Jankowski, R. [2005] "Non-linear viscoelastic modelling of earthquake-induced structural pounding," *Earthq. Eng. Struct. Dyn.* **34**, 595–611.

Khatami, M., Gerami, M. and Kheyroddin, A. [Publish in 19 March 2020] "Evaluation demand of separation gap angle in adjacent steel moment resisting frames under far-field and near-field earthquakes," *J. Civil Eng. Sharif.*

Mantawy, A. [2014] "Behavior of ductile reinforced concrete frames subjected to multiple earthquakes," Ph.D. thesis, Civil Engineering Dept., University of Southern California.

McKenna, F. and Fenves, G. [2007] *Open System for Earthquake Engineering Simulation* (University of California, Berkeley, USA).

Naderpour, H., Khatami, S. M. and Barros, R. C. [2017] "Prediction of critical distance between two MDOF systems subjected to seismic excitation in terms of artificial neural networks," *Period. Polytech. Civ. Eng.*, paper 9618.

Nazri, F. M., Miari, M. A., Kassem, M. M., Tan, C. G. and Farsangi, E. N. [2019] "Probabilistic evaluation of structural pounding between adjacent buildings subjected to repeated seismic excitations," *Arab. J. Sci. Eng.* **44**(5), 4931–4945.

PEER [2018] "Pacific Earthquake Engineering Research Center," Available at: https://peer.Berkeley.edu/peer ground motion database, Berkeley, USA.

SeismoSignal [2016] Earthquake Engineering Software Solutions (Version 5.1.2), Available at: https://www.seismosoft.com, Italy.

Shehata, E. and Raheem, A. [2014] "Mitigation measures for earthquake induced pounding effects on seismic performance of adjacent buildings," *Bull. Earthq. Eng.* **12**, 1705–1724.

Shrestha, B. [2013] "Effects of separation distance and nonlinearity on pounding response of adjacent structures," *Int. J. Civ. Struct. Eng.* **3**(3), 603–612.

Standard No. 2800 [2014] Road, Housing and Urban Development Research Center, in *Iranian Code of Practice for Seismic Resistant Design of Buildings (4th Edition)* (BHRC Publication, Iran).

Takabatake, H., Yasui, M., Nakagawa, Y. and Kishida, A. [2014] "Relaxation method for pounding action between adjacent buildings at expansion joint," *Earthq. Eng. Struct. Dyn.* **43**, 1381–1400.

Zhai, C. H., Wen, W. P. and Xie, L. L. [2012] "The influences of seismic sequence on the inelastic SDOF systems," *15th World Conference on Earthquake Engineering*, LISBOA.

Zhai, C. H., Wen, W. P., Chen, Z., Li, S. and Xie, L. L. [2013] "Damage spectra for the mainshock–aftershock sequence-type ground motions," *Soil Dyn. Earthqu. Eng.* **45**, 1–12.

Zhai, C. H., Wen, W. P., Li, S., Chen, Z., Chang, Z. and Xie, L. L. [2014] "The damage investigation of inelastic SDOF structure under the mainshock–aftershock sequence-type ground motions," *Soil Dyn. Earthq. Eng.* **59**, 30–41.